# Novel two-dimensional ferroelectric PbTe under tension: A first-principles prediction

Xilin Zhang,[1,2] Zongxian Yang,[2] and Yue Chen[1,a)]
[1]Department of Mechanical Engineering, The University of Hong Kong, Pokfulam Road, Hong Kong, China
[2]College of Physics and Materials Science, Henan Normal University, Xinxiang, Henan, China

(Received 10 June 2017; accepted 27 July 2017; published online 9 August 2017)

Enhanced ferroelectricity in two-dimensional (2D) SnTe exhibiting a higher transition temperature ($T_c$) than its bulk counterpart was recently discovered [Chang *et al.*, Science **353**(6296), 274–278 (2016)]. Herein, we report that nonferroelectric PbTe can be transformed into a ferroelectric phase by downsizing to two dimensions with suitable equi-biaxial tension. The crystal structure of the ferroelectric phase of 2D PbTe was determined using evolutionary algorithms and density functional theory. The dynamic stabilities of the predicted new phases were investigated using phonon calculations. To validate our results obtained using PbTe, we have also studied the ferroelectricity in GeTe and SnTe at the 2D level and compared them with the literature. The unequal lattice constants and the relative atomic displacements are found to be responsible for ferroelectricity in 2D GeTe, SnTe, and strained PbTe. This study facilitates the development of new 2D ferroelectrics via strain engineering and promotes the integration of ferroelectric devices. *Published by AIP Publishing.*
[http://dx.doi.org/10.1063/1.4989614]

## I. INTRODUCTION

Ferroelectric materials have received great attention because of their application in capacitors,[1] sonars,[2] and random access memory devices.[3] To meet the demands of miniaturization, a large number of experimental and theoretical studies have focused on the design and preparation of ultrathin films with stable ferroelectric properties.[4,5] Very recently, Chang *et al.* has reported stable in-plane spontaneous polarization in atomic-thick tin telluride (SnTe), down to a one-unit cell (UC) limit.[6] They reported that the one-UC SnTe film has much higher ferroelectricity than that of its bulk counterpart; this discovery may enable a wide range of applications in nonvolatile high-density memory devices, nanosensors, and electronics. Fei *et al.* reported that ferroelectricity in two-dimensional (2D) group-IV monochalcogenides MX (M = Ge, Sn; X = S, Se) is robust, and the corresponding transition temperature ($T_c$) is higher than the room temperature.[5] These studies indicate that reducing the size of ferroelectric materials to 2D may be a promising way to stabilize the ferroelectricity and increase the $T_c$ for the integration of ferroelectric devices.[7] The heavy group-IV monochalcogenide PbTe always exists as a nonferroelectric compound, because the $T_c$ of bulk PbTe is extrapolated to be below 0 K.[8] In this work, we report the stabilization of ferroelectricity in PbTe at the 2D level via strain engineering.

The global minimum crystal structures of GeTe, SnTe, and PbTe in 2D space were first determined by combining evolutionary algorithms[9] with density functional theory. Evolutionary algorithms have recently been shown to be extremely useful for the prediction of crystal structures with numerous successful applications.[10–12] Based on our predicted 2D crystal structures of GeTe and SnTe, we have successfully rationalized the experimentally observed enhanced ferroelectricity by comparing them to their bulk counterparts.[6] In addition, we found that the 2D global minimum crystal structures of GeTe and SnTe are extremely sensitive to the material thickness, whereas that of PbTe remains relatively unaffected by the thickness. The consistent theoretical and experimental results for GeTe and SnTe demonstrate the robustness of our approach. Motivated by these exciting findings, we further investigated PbTe, which is believed to be nonferroelectric at the 2D level.[6] The results showed that ferroelectricity cannot be introduced into PbTe by simply downsizing it to 2D, because no spontaneous polarization was observed, which is consistent with recent experiments.[6]

Strain engineering is an efficient method to enhance ferroelectricity.[13] Strain can be imparted to thin films by utilizing differences in the lattice parameter and the thermal expansion coefficient between the film and the underlying substrate, and has been widely adopted to manipulate the structural and electronic properties of various functional materials.[14–16] Recently, strain has been applied to induce ferroelectricity in some nonferroelectric compounds.[15] Choi *et al.* demonstrated that the strain imposed by coherent epitaxy can result in a $T_c$ nearly 770 K higher than that of the bulk $BaTiO_3$ single crystal.[17] Using first-principles calculations, Yang and coworkers[18] have also demonstrated that the spontaneous polarization of alkaline-earth-metal oxides increases with strain.

## II. COMPUTATIONAL DETAILS

The evolutionary algorithm implemented in USPEX[9] was employed to determine the global minimum crystal structures of 2D GeTe, SnTe, and PbTe. A maximum of 12 atoms were allowed in one unit cell. Thirty different 2D crystal structures were generated randomly in the first generation;

a)Author to whom correspondence should be addressed: yuechen@hku.hk

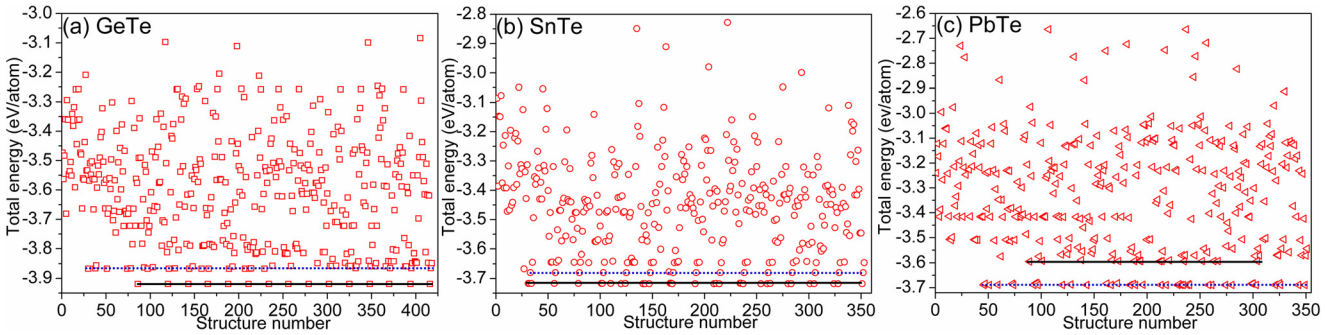


FIG. 1. The evolution of total energy of GeTe (a), SnTe (b), and PbTe (c) with respect to the structure number. The black and blue solid lines stand for the hexagonal and rippled crystal structures, respectively.

20 structures were generated based on the evolutionary algorithms in the subsequent generations. All the 2D crystal structures were fully optimized using the first-principles method as implemented in VASP.[19] The exchange-correlation energy was computed within the generalized gradient approximation[20] with the functional of Perdew, Burke, and Ernzerhof.[21] A plane-wave cutoff energy of 500 eV and a vacuum space of approximately 15 Å were applied. The Brillouin zones were meshed using the gamma-centered Monkhorst-Pack method for a density of about $2\pi \times 0.03$ Å$^{-1}$. The phonon dispersions were calculated using the finite displacement method as implemented in PHONOPY[22] to study the dynamic stabilities of the predicted new 2D crystal structures. A supercell of $7 \times 7 \times 1$ containing 196 atoms and a k-point mesh of $1 \times 1 \times 1$ were used to calculate the phonons. The energy convergence criterion of $10^{-8}$ eV was used for the self-consistent calculations to ensure accurate atomic forces.

## III. RESULTS AND DISCUSSION

The evolution of total energy with respect to the structure number is depicted in Fig. 1. Two most energetically preferable crystal structures, i.e., the hexagonal ($P\bar{3}m1$) and rippled structures ($Pmn2_1$ or P4/nmm), were identified for MTe (M = Ge, Sn, and Pb). These two crystal structures were found to be energetically more stable than the 2D structure sliced directly from the ground-state bulk structure with the R3m space group. The stable 2D crystal structure with thickness smaller than 3.5 Å is rippled, and is hereafter referred to as "ripp." The crystal structures and the corresponding unit cell parameters are shown in Fig. 2 and Table I, respectively. The phonon dispersions are shown in Figs. 2(c)–2(e) to verify the dynamic stabilities of these predicted 2D crystal structures. All the phonon frequencies are positive, indicating that all the studied 2D materials are dynamically stable.[23–25] The highest phonon frequency decreases gradually from GeTe through SnTe to PbTe following the increase in the atomic mass. From the unit cell parameters of GeTe and SnTe, as listed in Table I, we find that the lattice constant $a$ is smaller than $b$. A relative displacement between group-IV and Te atoms along the [010] direction is observed in GeTe and SnTe [see Fig. 2(a)]. This kind of relative displacement results in spontaneous polarization; in general, a larger relative displacement corresponds to a larger value of spontaneous polarization and leads to a higher $T_c$.[5] On the other hand, lattice constants $a$ and $b$ are equal in the case of 2D PbTe, and the relative displacement corresponding to spontaneous polarization is absent [see Fig. 2(b)]. Therefore,

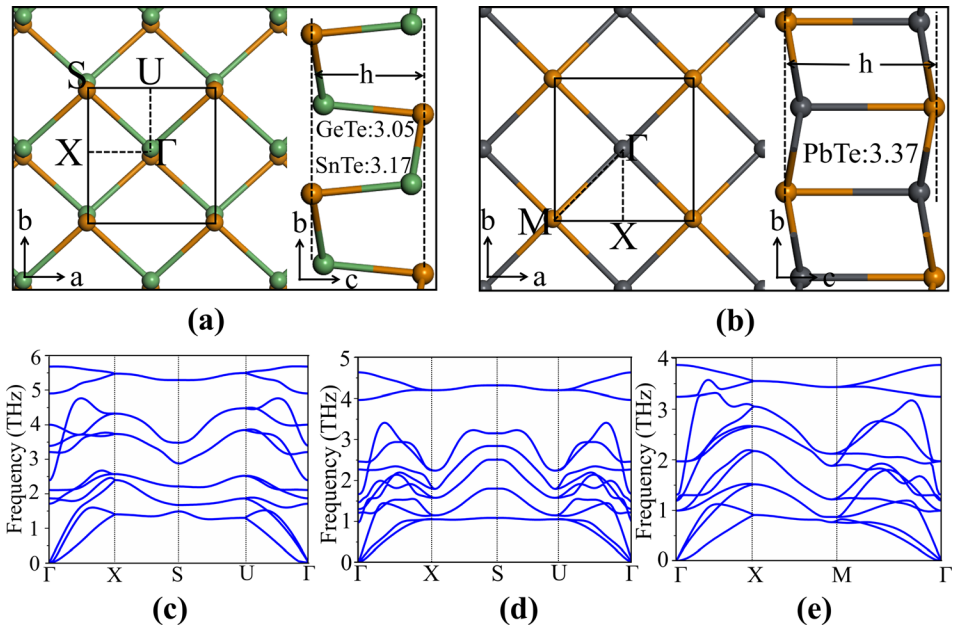


FIG. 2. The rippled crystal structures of 2D GeTe and SnTe in the $Pmn2_1$ space group (a), and 2D PbTe in the P4/nmm space group (b). High-symmetry points in the first Brillouin zones are labeled. Phonon dispersions of 2D GeTe ($Pmn2_1$) (c), SnTe ($Pmn2_1$) (d), and PbTe (P4/nmm) (e).

TABLE I. The key geometrical parameters of bulk MTe (M = Ge, Sn, and Pb) and 2D MTe with rippled crystal structures. The lattice constants (*a, b*, and *c*), the thickness *h*, the space group (SP), and the relative displacements between group-IV and Te atoms along the [010] and [111] directions for the 2D and bulk MTe, respectively (Dis). The ferroelectric bulk SnTe adopts the same crystal structure as GeTe.

| | Rippled | | | | | Bulk | | | |
|---|---|---|---|---|---|---|---|---|---|
| | a (Å) | b (Å) | h (Å) | SP | Dis (Å) | a (Å) | c (Å) | SP | Dis (Å) |
| GeTe | 4.24 | 4.39 | 3.05 | $Pmn2_1$ | 0.27 | 4.22 | 10.88 | R3m | 0.23 |
| SnTe | 4.55 | 4.58 | 3.17 | $Pmn2_1$ | 0.12 | 4.53 | 11.16 | R3m | 0.13 |
| PbTe | 4.64 | 4.64 | 3.37 | P4/nmm | 0 | 6.56 | 6.56 | $Fm\bar{3}m$ | 0 |

PbTe is still nonferroelectric at the 2D level, which agrees with recent experiments.[6] It is also evident from Table I that bulk GeTe has a larger relative atomic displacement than SnTe, whereas PbTe has no relative atomic displacement. The relative displacements are of the same order as that of the bulk ferroelectric $T_c$,[26] i.e., the larger the relative displacement, the higher the $T_c$. It is also seen that the relative atomic displacements in the 2D systems are comparable to those in the bulk materials. The experimentally observed more robust ferroelectricity of 2D GeTe and SnTe are potentially due to very different atomic environments from those in the bulk states.[6]

When the thickness of 2D MTe increases, the hexagonal crystal structure that belongs to the space group of P $\bar{3}$ m1 becomes more energetically preferable for GeTe and SnTe; this structure is hereafter labeled as "hex." The hex crystal structure and the corresponding unit cell parameters are shown in Fig. 3 and Table II, respectively. From the energetic point of view, the hex phases of GeTe and SnTe are more stable than the respective ripp phases; if the thicknesses of 2D GeTe and SnTe are larger than the one-UC limit, these compounds tend to adopt the hex crystal structure. The dynamic stabilities of the hex phases of GeTe and SnTe were also investigated using the phonon calculations. It is seen from Figs. 3(c) and 3(d) that no imaginary phonons are

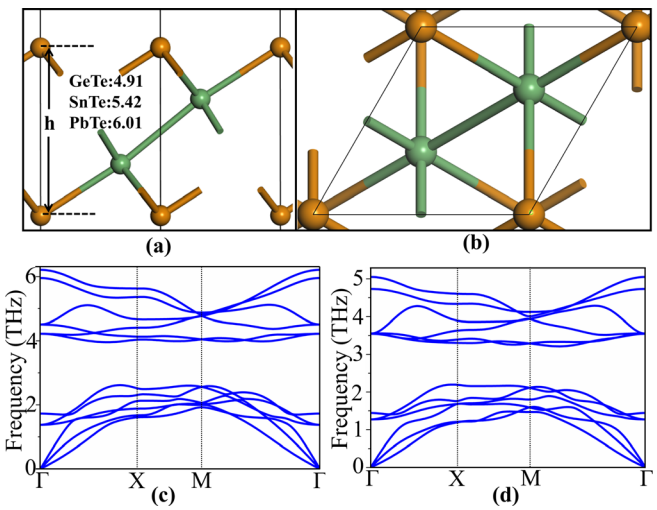


FIG. 3. Side view (a) and top view (b) of the hexagonal crystal structure in the P$\bar{3}$m1 space group. Phonon dispersions of 2D GeTe (c) and SnTe (d) in the hexagonal crystal structure.

TABLE II. The key geometrical parameters of 2D MTe (M = Ge, Sn, and Pb) with the hexagonal crystal structures. The lattice constants *a*, the thickness *h*, the space group (SP), and the energy differences between the 2D rippled and hexagonal crystal structures ($\Delta E = E_{ripp} - E_{hex}$). The data in the parentheses are taken from the literature.[27]

| | a (Å) | h (Å) | SP | ΔE (meV/atom) |
|---|---|---|---|---|
| GeTe | 4.06 (4.059) | 4.91 (4.896) | P$\bar{3}$m1 | 55 |
| SnTe | 4.33 (4.333) | 5.42 (5.416) | P$\bar{3}$m1 | 20 |
| PbTe | 4.43 (4.425) | 6.01 (6.008) | P$\bar{3}$m1 | −100 |

observed, indicating that these two phases are dynamically stable. In contrast, the hex phase of PbTe has a higher energy than the ripp phase, indicating that the ripp crystal structure is more stable [see Fig. 1(c)]. These results indicate that the crystal structures of 2D GeTe and SnTe are more sensitive to the thickness compared to 2D PbTe, which always prefers the ripp crystal structure in the thickness range studied in this work. Moreover, it is clear from Figs. 3(a) and 3(b) that the hex structure is centrally symmetric and nonferroelectric. Our results indicate that the ferroelectricity of 2D GeTe and SnTe is influenced by the thickness, i.e., it is necessary to achieve the one-UC limit to observe enhanced ferroelectricity in GeTe and SnTe.[6]

Most interestingly, we discover that ferroelectricity can be introduced in 2D PbTe by applying a suitable equi-biaxial tensile stress. Tensile stress was found to be effective in inducing ferroelectricity in nonferroelectric materials.[15,28] An *et al.* calculated the phonon dispersions of bulk PbTe under hydrostatic tensile strain, and speculated that a suitable strain may lead to a ferroelectric transition.[29] Nonetheless, the ferroelectric distortion discovered in the current work is different from that predicted in the bulk phase. In addition, 2D ferroelectric PbTe is more promising for practical applications, because equi-biaxial tensile stress can be more readily applied in two dimensions compared to inducing a hydrostatic tensile strain in bulk materials.[30] We find that the Born effective charge of Pb along the [010] direction decreases gradually from 5.46 to 3.02 as the equi-biaxial tension increases from 0 to ∼1.44 N/m [see Fig. 4(a)]. At tensions smaller than 0.80 N/m, lattice parameters *a* and *b* are equivalent, and no relative displacement between the Pb and the Te atoms is observed along the [010] direction, i.e., 2D PbTe is still nonferroelectric. Both the relative displacement and the difference in lattice constants *a* and *b* increase rapidly when the applied tension is larger than 0.80 N/m, indicating that the crystal structure of PbTe transforms from P4/nmm into $Pmn2_1$. The identical crystal structure of strained PbTe with those of 2D GeTe and SnTe suggests that suitable tension can induce ferroelectricity in PbTe. The relative atomic displacement along the [010] direction in 2D PbTe under a tension of about 1.08 N/m becomes comparable to that of 2D SnTe (∼0.12 Å), implying the robustness of ferroelectricity in 2D PbTe. The phonon dispersions of 2D PbTe under an equi-biaxial tension of 1.08 N/m are calculated and shown in Fig. 4(b). No imaginary phonons exist, indicating the dynamic stability of the $Pmn2_1$ phase of PbTe under the effect of strains. Our calculations predict that PbTe may be

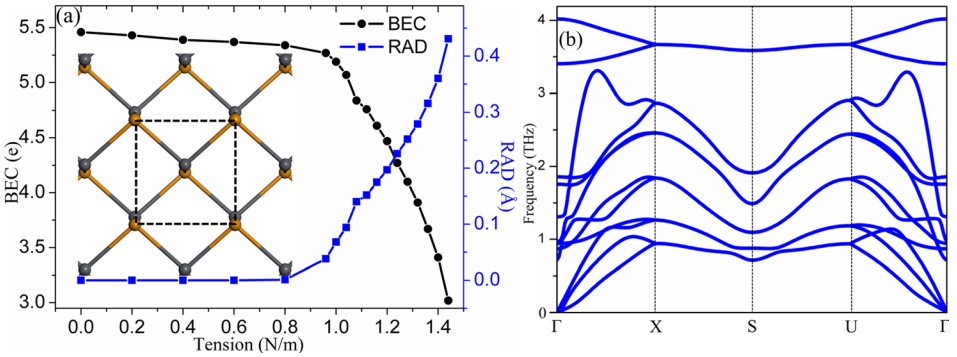


FIG. 4. The Born effective charge (BEC, black line) and relative atomic displacement (RAD, blue line) along the [010] direction as a function of tension (a); the phonon dispersions of the $Pmn2_1$ phase of 2D PbTe under a tension of 1.08 N/m (b).

stabilized in the ferroelectric phase by downsizing it to 2D and by applying suitable tensions.

## IV. CONCLUSIONS

In summary, the crystal structures and ferroelectricity of MTe (M = Ge, Sn, and Pb) at the 2D level are thoroughly investigated. The global minimum crystal structures of GeTe, SnTe, and PbTe in the 2D space are discussed with respect to different layer thicknesses. It is found that the stable crystal structure of GeTe and SnTe transforms from ferroelectric $Pmn2_1$ into nonferroelectric $P\bar{3}m1$, when the thickness is larger than the one-UC limit. In contrast, 2D PbTe always prefers the P4/nmm structure in the range of thickness considered in this work. A 2D ferroelectric phase of PbTe has been predicted to exist by applying suitable equi-biaxial tensile stress. It is found that the spontaneous polarization of 2D PbTe increases with increasing equi-biaxial tensions. Hence, the present study facilitates the development of new ferroelectric materials by downsizing it to 2D and the application of strain engineering in the miniaturization of ferroelectric devices.

## ACKNOWLEDGMENTS

We are grateful for the financial support of the Early Career Scheme of RGC under Project Number 27202516 and the research computing facilities offered by ITS, HKU. Z. Yang also acknowledges the support from the National Natural Science Foundation of China (Grant No. 11474086.)

[1]A. I. Khan, K. Chatterjee, B. Wang, S. Drapcho, L. You, C. Serrao, S. R. Bakaul, R. Ramesh, and S. Salahuddin, Nat. Mater. **14**, 182–186 (2015).
[2]K. T. Butler, J. M. Frost, and A. Walsh, Energy Environ. Sci. **8**, 838–848 (2015).
[3]S. James, P. Arujo, and A. Carlos, Science **246**, 1400–1405 (1989).
[4]D. A. Tenne, P. Turner, J. Schmidt, M. Biegalski, Y. Li, L. Chen, A. Soukiassian, S. Trolier-McKinstry, D. Schlom, and X. Xi, Phys. Rev. Lett. **103**, 177601 (2009).
[5]R. Fei, W. Kang, and L. Yang, Phys. Rev. Lett. **117**, 097601 (2016).
[6]K. Chang, J. Liu, H. Lin, N. Wang, K. Zhao, A. Zhang, F. Jin, Y. Zhong, X. Hu, and W. Duan, Science **353**, 274–278 (2016).
[7]A. V. Bune, V. M. Fridkin, S. Ducharme, L. M. Blinov, S. P. Palto, A. V. Sorokin, S. Yudin, and A. Zlatkin, Nature **391**, 874–877 (1998).
[8]K. M. Rabe and J. D. Joannopoulos, Phys. Rev. B **32**, 2302 (1985).
[9]C. W. Glass, A. R. Oganov, and N. Hansen, Comput. Phys. Commun. **175**, 713–720 (2006).
[10]H. Dong, A. R. Oganov, Q. Wang, S.-N. Wang, Z. Wang, J. Zhang, M. Esfahani, X.-F. Zhou, F. Wu, and Q. Zhu, Sci. Rep. **6**, 31288 (2016).
[11]E. McCalla, A. M. Abakumov, M. Saubanère, D. Foix, E. J. Berg, G. Rousse, M.-L. Doublet, D. Gonbeau, P. Novák, and G. Van Tendeloo, Science **350**, 1516–1521 (2015).
[12]Q. Wang, A. R. Oganov, O. D. Feya, Q. Zhu, and D. Ma, Phys. Chem. Chem. Phys. **18**, 19549–19556 (2016).
[13]K. J. Choi, M. Biegalski, Y. Li, A. Sharan, J. Schubert, R. Uecker, P. Reiche, Y. Chen, X. Pan, and V. Gopalan, Science **306**, 1005–1009 (2004).
[14]F. Guinea, M. Katsnelson, and A. Geim, Nat. Phys. **6**, 30–33 (2010).
[15]A. Vasudevarao, A. Kumar, L. Tian, J. Haeni, Y. Li, C.-J. Eklund, Q. Jia, R. Uecker, P. Reiche, and K. Rabe, Phys. Rev. Lett. **97**, 257602 (2006).
[16]R. Fei and L. Yang, Nano Lett. **14**, 2884–2889 (2014).
[17]D. D. Fong, G. B. Stephenson, S. K. Streiffer, J. A. Eastman, O. Auciello, P. H. Fuoss, and C. Thompson, Science **304**, 1650–1653 (2004).
[18]X. Yang, Y. Wang, H. Yan, and Y. Chen, Comput. Mater. Sci. **121**, 61–66 (2016).
[19]G. Kresse and J. Furthmüller, Phys. Rev. B **54**, 11169 (1996).
[20]S. Grimme, J. Comput. Chem. **27**, 1787–1799 (2006).
[21]M. Ernzerhof and G. E. Scuseria, J. Chem. Phys. **110**, 5029–5036 (1999).
[22]A. Togo, F. Oba, and I. Tanaka, Phys. Rev. B **78**, 134106 (2008).
[23]A. K. Singh and R. G. Hennig, Appl. Phys. Lett. **105**, 042103 (2014).
[24]L. Huang, F. Wu, and J. Li, J. Chem. Phys. **144**, 114708 (2016).
[25]O. Delaire, J. Ma, K. Marty, A. F. May, M. A. McGuire, M. H. Du, D. J. Singh, A. Podlesnyak, G. Ehlers, M. D. Lumsden, and B. C. Sales, Nat. Mater. **10**, 614–619 (2011).
[26]T. Chatterji, C. M. N. Kumar, and U. D. Wdowik, Phys. Rev. B **91**, 054110 (2015).
[27]B. Sa, Z. Sun, and B. Wu, Nanoscale **8**, 1169–1178 (2016).
[28]E. Bousquet, N. A. Spaldin, and P. Ghosez, Phys. Rev. Lett. **104**, 037601 (2010).
[29]J. An, A. Subedi, and D. J. Singh, Solid State Commun. **148**, 417–419 (2008).
[30]H. Hoshyarmanesh, N. Nehzat, M. Salehi, and M. Ghodsi, J. Mech. Sci. Technol. **29**, 715–721 (2015).